automation

MDPI

Article

Experimental Assessment of Control Loop Performance: A Methodology for Comparing On–Off and PID Actions in Dissolved Oxygen Regulation

Jose Magallanes [1,*], Styven Palomino [2], Anthony Gutarra [1] and Elvis Jara Alegria [1,*]

[1] Department of Electrical and Mechatronics Engineering, University of Engineering and Technology—UTEC, Lima 15063, Peru; agutarra@utec.edu.pe
[2] Department of Automation and Systems Engineering, Universidade Federal de Santa Catarina—UFSC, Florianopolis 88040-900, Brazil; styven.palomino@posgrad.ufsc.br
* Correspondence: jmagallanesc@utec.edu.pe (J.M.); ejara@utec.edu.pe (E.J.A.)

Abstract

Experimental validation of dissolved oxygen (DO) control in aquaculture is often limited by biological variability, environmental disturbances, and hydrodynamic complexity, which hinder reproducibility and reliable performance assessment. To address this, the present work proposes a laboratory-scale, control-oriented platform that minimizes external disturbances and enables experimentation under consistent conditions, supported by a statistically grounded methodology for performance evaluation. The platform integrates industrial-grade instrumentation and automated control hardware, ensuring reliable operation and practical relevance. Oxygen demand is emulated through chemical deoxygenation using sodium sulfite, allowing experiments to start from consistent near-zero DO conditions. Within this framework, On–Off and discrete-time PID controllers are implemented as baseline strategies to illustrate the methodology. Their evaluation through standard performance metrics and confidence-interval criteria illustrates how the platform can support rigorous, repeatable assessment of control actions. Rather than aiming at optimal control design, the proposed approach offers a benchmark methodology for dissolved oxygen regulation studies, providing a reproducible basis that may guide future investigations.

Keywords: dissolved oxygen control; experimental platform; aquaculture automation; PID control; On–Off control; programmable logic controller; aeration systems; reproducible experimentation

Check for updates

Academic Editor: Simone Fiori

Received: 18 February 2026
Revised: 8 May 2026
Accepted: 11 May 2026
Published: 19 May 2026

Copyright: © 2026 by the authors. Licensee MDPI, Basel, Switzerland. This article is an open access article distributed under the terms and conditions of the Creative Commons Attribution (CC BY) license.

1. Introduction

Efficient aquaculture production depends on maintaining water quality within suitable operational ranges. Key water parameters include pH, temperature, salinity, turbidity, and dissolved oxygen (DO), all of which directly affect metabolism, growth rate, feed conversion efficiency, and survival of cultured organisms [1,2]. Among these variables, dissolved oxygen is widely recognized as one of the most critical indicators of water quality [3,4]. Recent experimental studies on *Litopenaeus vannamei* have shown that insufficient DO availability induces physiological stress, tissue damage, metabolic alterations, growth depression, and reduced survival under hypoxic conditions [5,6], .

In aquaculture systems, the dynamics of DO are governed by the interaction of multiple coupled phenomena, including biomass respiration, organic matter degradation, hydraulic recirculation, mixing efficiency, aeration, and water temperature [3,7,8]. To mitigate

hypoxic events, several aeration technologies have been employed, including paddlewheel aerators, fine-bubble diffusers, venturi injectors, and mechanical surface aerators, each with distinct operational characteristics and oxygen transfer efficiencies [1,9,10]. However, their effectiveness depends not only on mechanical design but also on the control strategy applied and the availability of reliable DO feedback.

Accurate real-time measurement of dissolved oxygen is therefore a fundamental requirement for aquaculture automation. Conventional chemical methods, such as Winkler titration and colorimetric techniques, provide acceptable accuracy for spot analyses, but they are unsuitable for closed-loop control [11,12]. In contrast, electrochemical and optical DO sensors enable continuous digital monitoring and provide the feedback signals required for automatic control. Nevertheless, their practical performance depends on signal conditioning, calibration procedures, temperature compensation, communication reliability, and system-level integration [3,13,14].

Laboratory-scale experimental platforms have therefore become important tools for aquaculture research. These platforms, commonly implemented in recirculating configurations, are typically designed to replicate production scenarios and evaluate operational conditions such as organic loading, temperature fluctuations, and turbidity [15,16]. Although recent studies have proposed predictive models and adaptive control strategies for DO regulation in recirculating aquaculture systems [7,8,17], such platforms are often oriented toward production optimization and biological performance rather than toward the systematic evaluation of aeration-driven control dynamics under isolated conditions. Moreover, recirculating configurations inherently couple oxygen transfer with hydraulic residence time, recirculation flow, forced mixing, biological oxygen consumption, and organic loading, which makes it difficult to isolate the individual contribution of the aeration device and the control approach [7,8,14]. For this reason, a non-recirculating configuration can be advantageous, as it reduces external disturbances and allows DO regulation to be evaluated primarily as a function of aeration-induced bubble-plume dynamics.

Furthermore, conducting experimental studies using live organisms introduces inherent biological variability, which complicates the reproducibility and rigorous validation of control algorithms [18]. To address this limitation, some studies have proposed the use of chemical oxygen scavengers instead of living organisms, such as sodium sulfite, to induce controlled deoxygenation conditions in aquatic laboratory systems [18,19]. However, the practical implementation of sulfite-based deoxygenation requires careful consideration because the theoretical stoichiometry of the reaction may differ from real experimental conditions due to oxygen-transfer limitations, catalyst effects, water composition, temperature, and mixing-dependent oxidation kinetics [19,20]. Accordingly, this reaction should be applied with caution when used to generate reproducible deoxygenation profiles.

Based on these considerations, the present work introduces a laboratory-scale control-oriented testbed for the systematic study of aeration-driven DO dynamics. The platform integrates industrial-grade instrumentation, an aeration system, and a programmable logic controller to enable real-time monitoring and implementation of classical control strategies under controlled experimental conditions. By minimizing external disturbances, the framework allows DO regulation to be assessed primarily as a function of aeration input, thus supporting the implementation and experimental evaluation of conventional PID control without requiring adaptive compensation mechanisms within the present experimental scope. The main contribution is methodological: a reproducible experimental framework supported by consistent initial conditions, disturbance isolation, performance metrics, and experimental data intended to serve as a benchmark for future studies on modeling and advanced control strategies in smart aquaculture.

In summary, the contributions of this work are:

- Design and implementation of a laboratory-scale DO control platform.
- A reproducible experimental methodology for benchmarking DO control strategies.
- Experimental validation and statistical framework.

The remainder of this article is structured as follows. Section 2 describes the proposed experimental framework, including the design and construction of the laboratory-scale platform, the instrumentation employed, and the management methodology adopted. This section also details the control design and the experimental validation procedure. Section 3 presents the experimental results and discussions obtained under controlled operating conditions. Finally, the conclusions are presented in Section 4.

2. Materials and Methods

Our proposed framework is structured into three main stages with the objective of developing and validating a laboratory-scale experimental platform for the analysis and control of dissolved oxygen dynamics under reproducible conditions.

2.1. Experimental Platform and Management Methodology

This section addresses the design of a controlled experimental test bed integrating the process tank, aeration system, sensing and actuation hardware, and a programmable logic controller (PLC). A management methodology is defined to ensure repeatable operating conditions, including chemical DO depletion and standardized operating procedures. Data acquisition and signal conditioning are performed to provide reliable measurements for control-oriented analysis.

2.1.1. Physical Platform and Instrumentation Design

The experimental platform was conceived as a laboratory-scale, control-oriented test bed aimed at the systematic evaluation of DO control strategies under well-defined and repeatable conditions. Its architecture intentionally isolates the aeration process, allowing DO dynamics to be studied without the confounding effects typically present in full-scale aquaculture systems.

The main structure of the system is a rigid process tank (Figure 1), operating at a fixed working volume of 160 L. Together with the aerators and the DO sensor, this tank constitutes the core of the process in which DO concentration must be controlled. Water inflow is enabled only during preparation stages via the inlet line controlled by valve VS1, while discharge occurs exclusively during cleaning and reset procedures through valve VS2 and a water output pump. Since recirculation is excluded during closed-loop operation, both inflow and outflow remain inactive.

Compressed air supplied by a pneumatic subsystem contains not only oxygen but also nitrogen, carbon dioxide, argon, and other trace gases. However, in the following analysis only oxygen is considered as the variable of interest. As shown in Figure 1, air is delivered by a compressor operating at a pressure of 3.5 bar. The stream passes through a flow control valve (FV1) and a check valve before reaching the submerged diffusers located at the bottom of the tank.

During preparation, sodium sulfite is manually added to the tank to induce controlled oxygen depletion. After preparation, dissolved oxygen was measured in real time using the Aqualabo OPTOD sensor (AQUALABO, Champigny-sur-Marne, France), which operates with luminescent optical technology. Immersed in the tank, it provides the primary feedback variable for control. In this stage, a small amount of residual sulfite may remain and act as a transient oxygen-demand disturbance during closed-loop control. As shown in Figure 2, a programmable logic controller (Allen Bradley Micro 870, Rockwell Automation,

Milwaukee, WI, USA) acquires these measurements via an RS-485 interface and executes the discrete-time control algorithm, generating actuation commands to FV1.

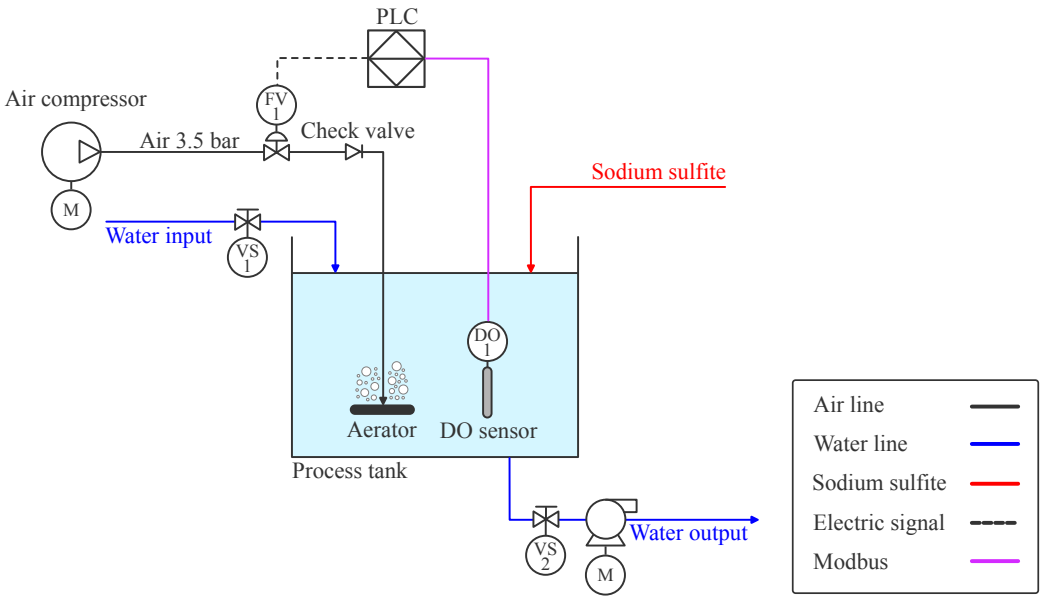


Figure 1. Functional architecture and integrated air, water, and signal flows of the experimental DO control platform.

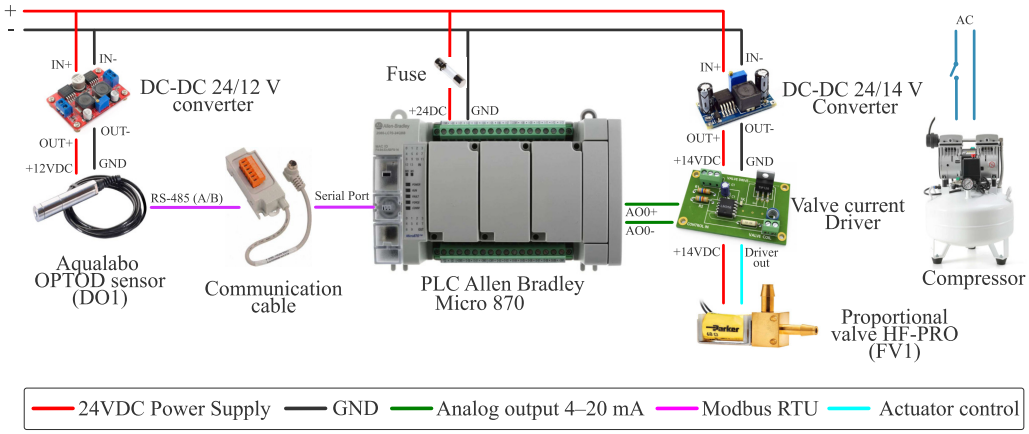


Figure 2. Control and instrumentation architecture of the experimental DO control platform.

The analog control signal generated by the PLC is conditioned by a valve current driver and applied to an electropneumatic proportional valve (HF-PRO, Parker Hannifin, Cleveland, OH, USA), which regulates the airflow supplied by the compressor to the submerged diffusers and constitutes the final control element of the aeration loop. The electrical architecture supporting the control loop is centralized around a 24 VDC power supply. Dedicated DC-DC converters generate the voltage levels required by the sensor, valve driver, and auxiliary components, while protective elements such as fuses are also included.

A summary of the main instrumentation and hardware specifications, including the key dimensioning parameters required for experimental replication, is provided in Table 1.

Together, Figures 1 and 2 provide complementary views of the experimental platform, combining a process-oriented representation of air, water, and signal flows with an implementation-level description of the control, instrumentation, and power architecture supporting reproducible experimental validation of DO control strategies.

Table 1. Main instrumentation and hardware specifications of the experimental DO control platform.

Element	Key Specifications	Function in the System
Process tank	Rigid tank, 160 L working volume; laboratory-scale geometry; single-phase liquid operation.	Physical process where dissolved oxygen dynamics are regulated.
Aerators	Submerged air diffusers; porous stone type; characteristic pore size in the sub-millimeter range; installed symmetrically at the tank bottom; nominal airflow ≈ 1–3 L/min per aerator.	Promote gas–liquid oxygen transfer and spatially uniform aeration.
Air compressor	Oil-free air compressor; Set to a pressure of 3.5 bar; air tank capacity ≈ 40 L; nominal flow capacity ≈ 160 L/min.	Provides pressurized air to the aeration subsystem.
Flow control valve (FV1)	Proportional valve; 2-way normally closed; maximum flow up to ≈60 SLPM; operating pressure up to 3.5 bar; current-driven actuation (0–175 mA).	Final control element regulating aeration rate.
Valve driver	Analog current driver; PLC-compatible input; valve supply voltage 12–14 VDC; maximum output current ≈ 200 mA.	Conditions the PLC output to drive the proportional valve.
DO sensor	Optical dissolved oxygen probe; measurement range 0–20 mg/L; accuracy ± 0.1 mg/L; Modbus RS-485 communication; integrated temperature compensation.	Provides real-time DO measurements for feedback control.
Controller	Programmable Logic Controller (PLC); discrete-time execution; analog output (4–20 mA); serial communication via RS-485 (Modbus).	Executes the closed-loop DO control algorithm.
DC power conversion	DC-DC converters; 24 VDC main supply stepped down to 12 VDC and 14 VDC; current capacity up to 3 A.	Supplies regulated power to valve driver and instrumentation.

2.1.2. Platform Operation & Management Methodology

A structured operating and management methodology was defined to ensure repeatability, consistency, and traceability across experimental trials. The overall workflow adopted for the use of the experimental platform is summarized in the operational flow diagram, as shown in Figure 3, which outlines the preparation, control execution, and reset stages of each experiment.

Each experimental run begins with a preparation phase, during which the process tank is filled to the nominal operating volume of 160 L. The PLC program is then deployed and executed, and correct acquisition of dissolved oxygen (DO) measurements from the sensor is verified before enabling any control action. During this phase, the system remains in preparation mode to prevent unintended aeration.

To establish a reproducible initial condition and emulate the oxygen consumption typically caused by biological activity in aquaculture systems, a chemical oxygen depletion procedure is applied. A fixed amount of 12 g of sodium sulfite (Na_2SO_3) is manually added to the water. This compound reacts chemically with dissolved oxygen, progressively reducing the DO concentration until an anoxic condition is reached. It is worth noting that the natural decrease in DO, considering the maximum volume and initial aeration of the water, takes approximately 30 to 40 min. To accelerate this process, manual stirring was performed, reducing the DO level in less than 10 min. The number of manual mixing attempts ranged between four and five. Once the DO value approached zero, the water was allowed to rest for two minutes to stabilize the measurement. In this proposal, the deoxygenation

step was standardized only to achieve a consistent low-DO initial condition because the controlled aeration phase was the primary focus.

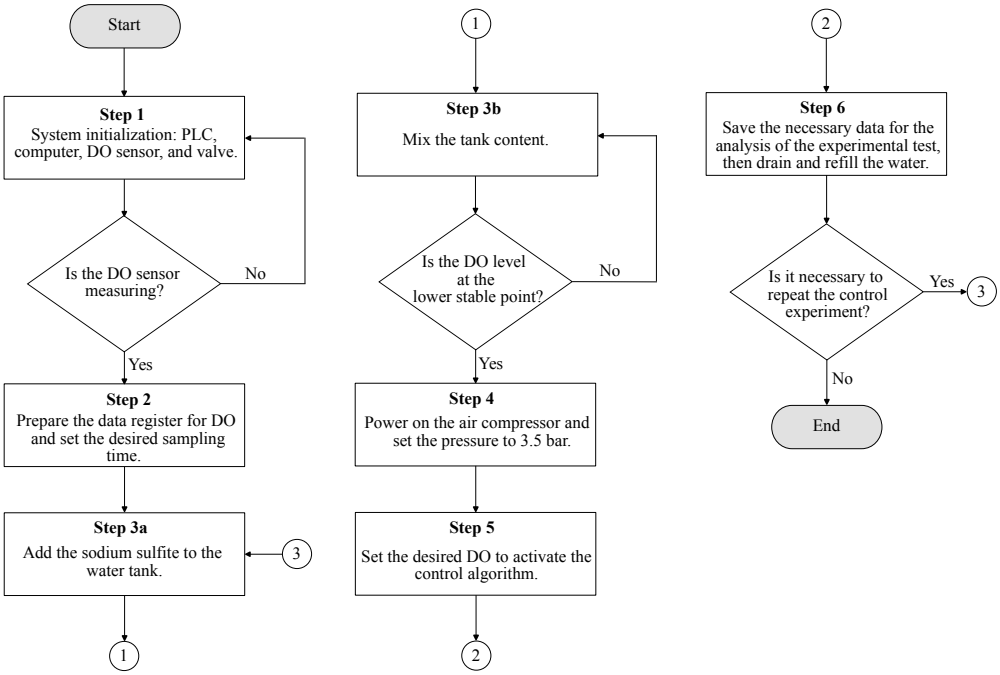


Figure 3. Operational workflow for experimental execution on the DO control platform.

Once the target low-DO condition is achieved, the system transitions to the control execution phase. The selected control algorithm is activated within the PLC, and the platform operates in closed loop. During this phase, aeration is driven exclusively by the controller output. DO measurements and control signals are acquired in discrete time at a fixed sampling period T_s and logged continuously for subsequent analysis.

After completion of each experimental run, a reset phase is performed. The aeration system is deactivated, the process tank is drained, and both the tank and the DO sensor are cleaned to remove residual sodium sulfite and prevent cross-test interference. This procedure ensures consistent initial conditions for successive experiments.

All data acquisition and signal handling are performed within the PLC. Raw DO measurements are internally scaled to engineering units before being used in control computations. To reduce the influence of measurement noise and short-term fluctuations inherent to dissolved oxygen sensing, a low-order digital filter is applied to the measured signal prior to its use in the control law. Both filtered and unfiltered signals are stored, allowing transparent offline analysis without affecting real-time execution.

Overall, this operating methodology ensures that experimental results are obtained under controlled and repeatable conditions, supporting the use of the platform as a laboratory-scale test bed for the experimental validation of dissolved oxygen control strategies.

2.2. Chemical Reduction of Dissolved Oxygen Using Sodium Sulfite

The proposed platform is designed to increase DO via aeration. Because it does not incorporate hardware to actively decrease DO (e.g., inert-gas sparging, vacuum degassing, or dedicated deoxygenation modules), a chemical oxygen scavenger was used to establish low-DO conditions for testing. Following standard practice for preparing a zero-DO solution for sensor calibration and low-oxygen checks, sodium sulfite (Na_2SO_3) was selected as the reducing agent [21]. In aqueous media, sulfite consumes dissolved oxygen and is oxidized to sulfate according to:

$$Na_2SO_3 + \tfrac{1}{2}O_2 \rightarrow Na_2SO_4. \quad (1)$$

Thus, the theoretical stoichiometry requires 1 mol of Na_2SO_3 per 0.5 mol of O_2 removed. For a water volume $V = 160$ L, the stoichiometric mass of sodium sulfite in grams needed to remove an initial DO concentration C_{DO} (g·L^{-1}) can be expressed as:

$$m_{Na_2SO_3} = \left(\frac{C_{DO}\, V}{32}\right) \times 2 \times 126 \quad (2)$$

where 32 is the molar mass of O_2 in g·mol^{-1} and 126 g·mol^{-1} is the molar mass of Na_2SO_3. In practice, the sulfite was added under mixing until the DO approached the target low level, and the final requirement was adjusted experimentally.

Implications of Using Potable Water (Chlorine Demand and Correction of the Theoretical Dose)

Potable water was used (160 L), which introduces an important practical correction: Na_2SO_3 reacts not only with dissolved oxygen, but also with oxidants present in disinfected drinking water (e.g., free chlorine and chloramines). This additional demand can increase the required sulfite mass beyond the oxygen-only stoichiometric estimate in Equation (2). The reactivity of sulfite toward chlorine species and the broader implications of sulfite-based dechlorination/quencher chemistry have been documented in peer-reviewed studies [22–24]. Therefore, rather than relying solely on stoichiometry, the sulfite dose was determined using a two-step approach:

1. Initial stoichiometric estimate: Compute the oxygen-only requirement from Equation (2) using the measured initial DO.
2. Experimental correction in potable water: Apply the estimated dose under agitation and verify whether the measured DO reaches the intended low value. If not, add incremental sulfite until the target DO is achieved, thereby capturing the additional oxidant demand of the potable water matrix [22–24].

This correction is consistent with the fact that sulfite scavenges dissolved oxygen (rather than reacting with water molecules), while still potentially consuming residual disinfectants and interacting with trace constituents in real waters [22,24].

2.3. Data Acquisition, Pre-Processing, and Control

The aeration control system begins with sampling the signal to determine the preprocessing of the measurements, which establishes the basis for the subsequent control actions. It considers mainly a desired dissolved oxygen setpoint (DO_d), a controller, a process, a DO sensor, and an IIR filter, as shown in Figure 4. The implementation treats the process model as a black-box, where the input is the control effort, represented by the valve aperture, with a maximum value limited by the 3.5 bar threshold of the valve—see Table 1—while the output is the DO measurement.

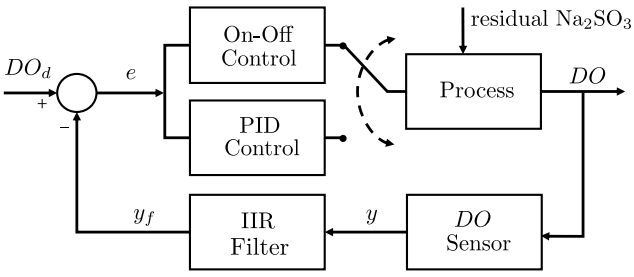


Figure 4. Block diagram of the feedback aeration control system.

2.3.1. Sampling and Preprocessing of Dissolved Oxygen Measurements

The experiments were conducted under controlled laboratory conditions using the experimental platform described in Section 2.1.2. The water temperature was maintained at approximately 20–21 °C, and a fresh volume of potable water was supplied for each run. The DO sensor was positioned 12 cm from the tank border with an immersion depth of 20 cm, while two diffusers were fixed at the base in equidistant positions on opposite sides. During each measurement, both the inlet and outlet valves remained closed to ensure stable hydraulic conditions.

Under our laboratory conditions, the initial DO measurements ranged from 0 to 7.8 mg/L. Each aeration experiment lasted 1 h and 15 min, whereas the DO depletion phase exhibited variable duration, being terminated once the concentration approached zero.

For the DO measurement $y[k]$ at discrete instants $k = 1, 2, \ldots, k_{\max}$, a first-order infinite impulse response (IIR) filter was implemented to attenuate noise by smoothing the experimental data [25]. The discrete-time representation of the filter is given in Equation (3):

$$y_f[k] = \alpha\, y_f[k-1] + (1-\alpha)\, y[k] \tag{3}$$

where $y_f[k]$ denotes the filtered output at instant k, and α is a forgetting factor close to one that determines the relative weight of past and current measurements [26]. Henceforth, the filtered signal y_f will be employed in our analysis during both the DO decay stage and the controlled aeration stage. For simplicity, y_f will be referred to as DO, whereas y will denote the raw DO measurement.

For the controlled aeration stage using PID, an experiment is required to obtain a reaction curve, which is subsequently described in Section 2.3.3. To this end, a sigmoidal adjustment is proposed y_{sig} by means of a logistic function:

$$y_{\text{sig}}(t) = \frac{L_\infty}{1 + e^{-\kappa(t-t_0)}} \tag{4}$$

where L_∞ denotes the maximum asymptotic value, κ the slope parameter, and t_0 the inflection point of the curve. To estimate these parameters, the following cost function is minimized using the least squares method $J(L_\infty, \kappa, t_0) = \sum_{k=1}^{k_{\max}} \left(y_f[k] - y_{\text{sig}}(k) \right)^2$. Therefore, the optimal parameters are $(L_\infty^*, \kappa^*, t_0^*) = \arg\min_{L_\infty, \kappa, t_0} J(L_\infty, \kappa, t_0)$.

The logistic function is used as a smooth approximation of the reaction curve to facilitate parameter extraction for Ziegler–Nichols tuning.

2.3.2. On–Off Control Design

In aquaculture systems, advanced control methods are often required due to external disturbances and complex coupled dynamics [27–30]. In contrast, the proposed testbed minimizes such disturbances, simplifying the plant model so that conventional control strategies provide a suitable baseline for reproducible performance evaluation.

As part of the control strategies, an On–Off controller is proposed. This approach ensures low computational cost and straightforward implementation. The controller operates by switching between open and closed states according to the sensor measurement relative to the reference value [31].

This control strategy employs hysteresis, which prevents excessive switching and thereby protects the equipment during tests. The hysteresis band $[-H, H]$ (mg/L) is determined by control requirements, as well as by the characteristics of the sensor, actuator, and volume of water. The valve aperture ($u_{\text{On-Off}}$) is fully open when the filtered DO value (y_f) is below the desired value (DO_d), and fully closed when the measurement exceeds the desired value, as detailed below.

$$u_{\text{On-Off}}(k) = \begin{cases} 100\%, & \text{if } y_f(k) \leq DO_d - H \\ u_{\text{On-Off}}(k-1), & \text{if } DO_d - H < y_f(k) < DO_d + H \\ 0\%, & \text{if } y_f(k) \geq DO_d + H \end{cases} \quad (5)$$

The implementation of this controller considers only the positive error, leading to the oxygen inflow. In this case, this characteristic is suitable because the proposed system does not extract oxygen. In terms of safety, the correct selection of hysteresis protects the system electrically and mechanically.

2.3.3. PID Controller Design via Ziegler–Nichols Method

The continuous-time control law implemented for the PID controller is given by

$$u_{\text{PID}}(t) = k_p e(t) + k_i \int_0^t e(\tau)\, d\tau + k_d \frac{de(t)}{dt}, \quad (6)$$

where $u_{\text{PID}}(t)$ denotes the valve aperture, $e(t)$ is the control error, and k_p, k_i, and k_d are the proportional, integral, and derivative gains, respectively.

For implementation purposes, the control law is discretized using a fixed sampling time T_s, which is independent of the specific hardware platform employed. The discrete-time representation of the PID controller is expressed as

$$u_{\text{PID}}[k] = k_p \left(e[k] + \frac{T_s}{T_i} \sum_{i=0}^{k} e[i] + \frac{T_d}{T_s} \left(e[k] - e[k-1] \right) \right), \quad (7)$$

where T_i denotes the integral time (s) and T_d denotes the derivative time (s).

The tuning of the PID controller is performed using the Ziegler–Nichols (ZN) method [31–33]. The procedure involves fitting the experimental data of a system reaction curve to a sigmoidal function, which is obtained from a step input experiment with amplitude m—see Figure 5 (left)—combined with data treatment based on filtering and sigmoidal fitting as shown in Section 2.3.1.

Two key parameters of this sigmoidal curve must be determined geometrically: the delay time (L) and the time constant (T). The slope of the tangent at the inflection point defines the reaction rate (R), with $R = A/T$; see Figure 5 (right).

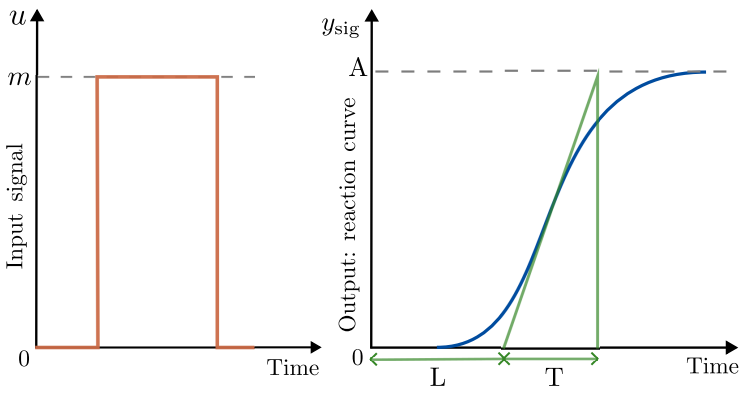


Figure 5. Step input signal (**left**) and corresponding reaction curve with Z-N parameters (**right**).

The relationship between the Ziegler–Nichols parameters and the controller gains is given by $k_p = \frac{1.2m}{RL}$, $T_i = 2L$, and $T_d = 0.5L$. It is worth mentioning that the classical Ziegler–Nichols method employs a first-order plus dead-time approximation of the reaction curve. In our case, however, a sigmoidal fitting was adopted since it provided a more consistent representation of the experimental data.

It is worth mentioning that the logistic function employed in this study is not intended to represent the underlying physical dynamics of the system, nor to serve as a predictive model for simulation purposes. Instead, it is introduced as a smooth and analytically tractable approximation of the experimentally obtained reaction curve. This approximation enables a more robust and consistent extraction of characteristic parameters required for the application of the Ziegler–Nichols tuning method. By reducing the influence of experimental noise and irregularities in the measured data, the logistic fit improves the reliability of the parameter identification process.

2.4. Statistical Criterion for Determining the Number of Experimental Repetitions

The control system is evaluated using standard performance metrics: overshoot, rise time t_r, defined as the time required for the measured DO concentration to increase from 10% to 90% of the reference value, settling time t_s, defined as the time required for the DO concentration to enter and remain within a $\pm 5\%$ band around the reference, and the mean steady-state error e_{ss}, calculated as $e_{ss} = \frac{1}{k_{\max}} \sum_{k=1}^{k_{\max}} e(k)$, where $e(k) = DO_d - y_f(k)$ (mg/L) denotes the instantaneous error at sample k once the system has reached steady state, and $k_{\max}$ is the number of samples considered in that regime.

In order to determine the number of repetitions required to obtain a statistically reliable estimate of the steady-state mean error e_{ss}, a confidence-interval-based precision criterion was adopted [34]. Let $e_{ss,i}$ denote the mean steady-state error obtained in the i-th experiment. Therefore, the mean error of N independent repetitions, denoted by $\bar{e}_{ss,N}$ is defined as

$$\bar{e}_{ss,N} = \frac{1}{N} \sum_{i=1}^{N} e_{ss,i}. \tag{8}$$

Therefore, the corresponding standard deviation of the experiments is

$$s_N = \sqrt{\frac{1}{N-1} \sum_{i=1}^{N} (e_{ss,i} - \bar{e}_{ss,N})^2}, \tag{9}$$

such that the standard error of the mean is defined as

$$SE_N = \frac{s_N}{\sqrt{N}}. \tag{10}$$

Assuming approximate normality of the estimator, a two-sided 95% confidence interval (CI) for the true mean error is computed using the Student's t distribution, that is, $\bar{e}_{ss,N} \pm h_N$, with $h_N = t_{0.975,\,N-1}\, SE_N$, where $t_{0.975,\,N-1}$ denotes the critical value with $N-1$ degrees of freedom. The quantity h_N represents the semi-width of the confidence interval and provides a direct measure of estimation precision [35].

Therefore, a practical stopping criterion can be defined by selecting the minimum number of repetitions N such that $h_N \leq \varepsilon$, where ε is a predefined tolerance on the admissible uncertainty of the estimated mean error [34].

3. Results and Discussions

3.1. Implementation of the Experimental Platform and Management Methodology

The experimental platform developed in this work was successfully implemented and operated as a laboratory-scale test bed for DO control experiments. The final system integrates the process tank, pneumatic aeration subsystem, sensing instrumentation, control hardware, and power distribution into a compact and functional structure, as shown in Figure 6. The implemented platform is consistent with the proposed design and enabled systematic experimentation under controlled conditions.

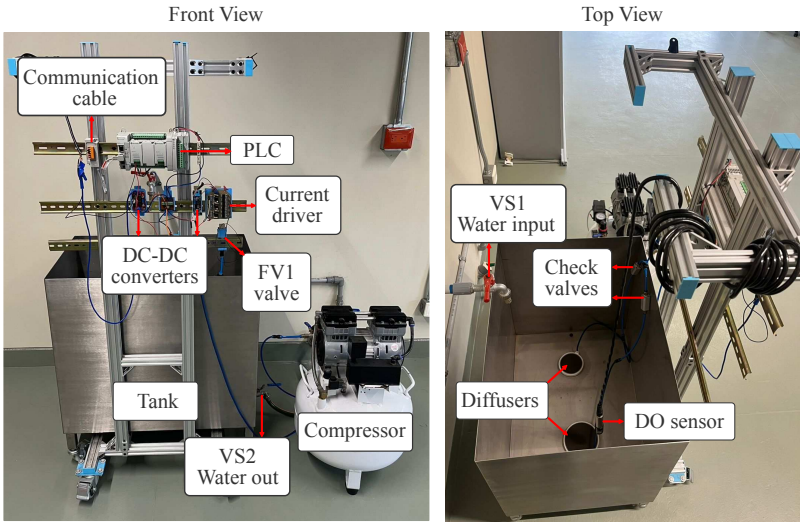


Figure 6. Implemented experimental platform for dissolved oxygen control experiments: front and top views.

The process tank operated at a nominal working volume of 160 L in all experimental trials. Water handling components allowed reliable filling and draining between experiments, while the pneumatic subsystem operated without mechanical faults, providing consistent air delivery during closed-loop operation.

The sensing and control infrastructure functioned reliably throughout the experiments. The optical DO sensor provided continuous measurements and stable RS-485 communication with the PLC ensured uninterrupted data acquisition. Control execution within the PLC was performed in discrete time, with actuation commands continuously applied to the proportional valve.

The chemical oxygen depletion procedure based on the manual addition of 12 g of sodium sulfite (Na_2SO_3) consistently reduced the DO concentration to low levels prior to control activation. Similar depletion behavior was observed across repeated trials, confirming the reproducibility of the selected dosing and mixing procedure.

Transitions between preparation, closed-loop operation, and reset phases were achieved without operational discontinuities. The reset procedure, involving tank draining and sensor cleaning, enabled recovery of comparable initial conditions between experiments. Dissolved oxygen measurements, control signals, and time stamps were logged continuously in all trials, supporting offline analysis. Basic signal conditioning reduced short-term measurement fluctuations while preserving the dominant process dynamics.

Overall, the obtained results confirm that the implemented platform and its associated management methodology provide a reliable and reproducible laboratory-scale environment for the experimental validation of dissolved oxygen control strategies.

3.2. Results of Dissolved Oxygen Control

Considering the platform above, this work uses the two mentioned controller methods to compare the results under the same conditions. The objective of each test is to track a desired DO level by regulating the valve aperture. The sensor measurements were filtered using an IIR filter with a forgetting factor of $\alpha = 0.95$. In this system, the increase in DO is determined by the valve, while sulfite determines the drop. Before control initialization, the DO level was reduced to a value close to zero by adding 12 g of sodium sulfite, exceeding the 9.3 g required by stoichiometry, due to the use of potable water instead of pure water, as described in Section 2.2.

While DO dynamics are often described in the literature using ODE-based mechanistic models, these approaches generally require the estimation of process-dependent param-

eters and measurable state variables. Such models provide a mathematically rigorous and physically interpretable representation of DO behavior and are useful for simulation, theoretical analysis, and control-oriented studies [17]. However, their accurate implementation under real experimental conditions may be limited when key parameters or variables are not directly measurable. In the present setup, this limitation is particularly relevant because the deoxygenation mechanism relies on sodium sulfite addition, whose effective behavior is affected by incomplete mixing, transient concentration gradients, and variability introduced by manual agitation. As a result, the effective oxygen demand and reaction conditions are not directly observable. A fully parameterized ODE-based model would therefore require additional instrumentation to measure or estimate key variables, such as local concentration distributions, reaction rates, and mass-transfer-related effects, which are not available in the present experimental setup [8]. For this reason, rather than suggesting that ODE-based models are inadequate, this study adopts a reproducible experimental identification approach based directly on measured data and controlled initial conditions. This approach provides a practical representation of the dynamics relevant to the proposed control evaluation framework.

Furthermore, the reduction in DO also depends on the initial DO value, which itself is influenced by the water flow rate when filling the tank. Figure 7 (left) illustrates three examples of DO reduction from a high initial value. In Test 1, a typical decay is observed without water agitation. In Tests 2 and 3, the reduction occurs more rapidly due to agitation. However, in Test 2, a slight increase can be observed after 0.2 h, caused by aeration generated by water agitation. Altogether, these observations highlight the need to conduct experiments under the same initial DO condition, close to zero, prior to controlled aeration evaluated in Sections 3.2.1 and 3.2.2, in order to reach repeatability under laboratory conditions.

Due to the empirical adjustment of the sodium sulfite dosage, it is not possible to determine with certainty whether residual sulfite remains in the water when near-zero DO conditions are reached, and therefore whether it continues to react during the initial aeration phase. Figure 7 (right) illustrates a typical aeration process under such excess conditions (about 20 g), where sodium sulfite reacts immediately upon air introduction, producing abrupt changes in the DO measurement from the outset, as both the increase in DO and the simultaneous consumption of sodium sulfite occur together.

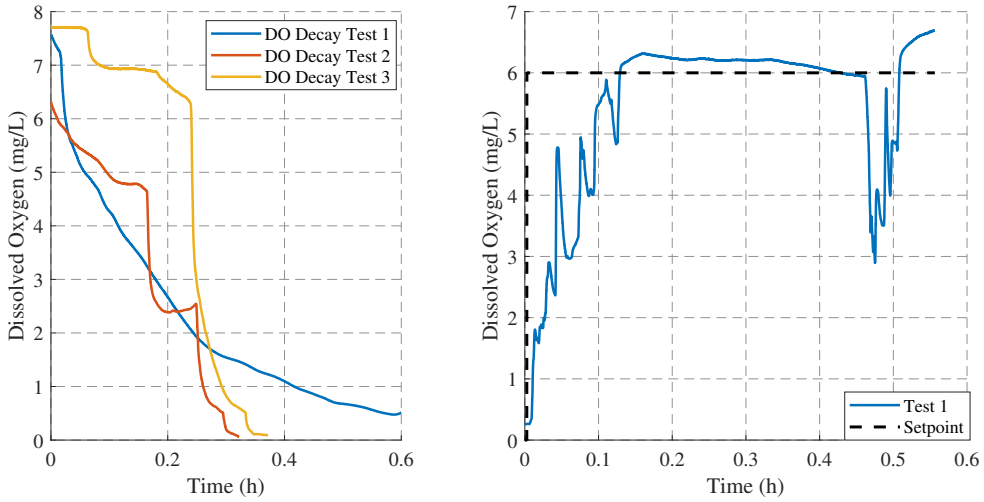


Figure 7. Example of three typical DO decay curves, starting from the high values characteristic of freshly collected drinking water and decreasing to a minimum due to reaction with sodium sulfite (**left**), and typical DO evolution when an excessive amount of sodium sulfite (about 20 g) is added (**right**).

For both control approaches, this study performed 10 tests for each to evaluate the consistency of their responses.

3.2.1. Results of the On–Off Control Strategy

The On–Off control employs 5% hysteresis with respect to $DO_d = 6$ mg/L (i.e., $H = 0.3$ mg/L). In this case, the 10 tests last approximately 1.3 h to track the DO setpoint. Sodium sulfite provides a repeatable oxygen demand disturbance that reduces DO in the bench system. This controller provided a fair response in tracking the reference throughout the test. In Figures 8 and 9, note that the peaks reached in each test are produced due to the delay effect of the aerator. The DO level continues to rise despite the control valve being completely closed. Conversely, the minimum peak corresponds to the drop in DO caused by the sulfite reaction when the valve is opened to regulate the DO level.

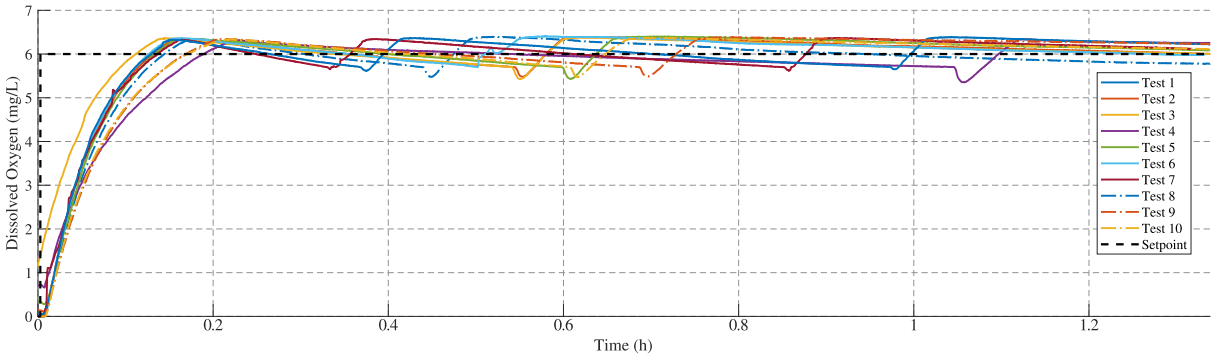


Figure 8. Dissolved oxygen responses obtained with On–Off control over 10 repetitions at a setpoint of 6 mg/L.

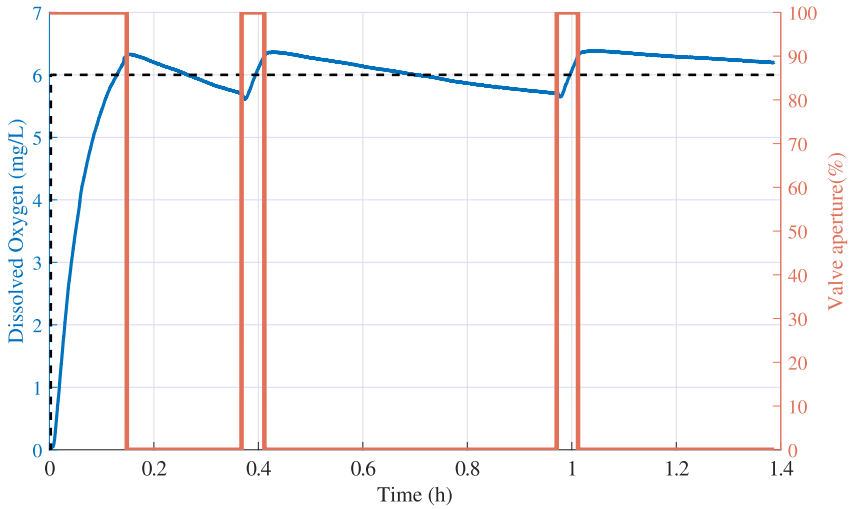


Figure 9. Corresponding valve aperture (orange line) for Test 1 under On–Off control (blue line) and reference (dashed line).

Table 2 summarizes the performance obtained in each test using the proposed controller. In terms of overshoot, the average is 47.4×10^{-2} (mg/L), with a maximum of 93.6×10^{-2} (mg/L) in test 5 and a minimum of 34.2×10^{-2} (mg/L) in test 4. The settling time has an average of 451.4 s (0.125 h) with a minimum of 339 and a maximum of 595 at tests 3 and 4, respectively. On the other hand, the average rising time is 355.4 s (0.099 h), with a maximum of 523.5 at test 4 and a minimum of 291 at test 3. Finally, the maximum mean error was observed in test 5, while the minimum occurred in test 10. These On–Off

control performance results can be adjusted depending on the value of the hysteresis band H [31].

Table 2. Test results and average performance of the On–Off Control.

Test	Overshoot ($\times 10^{-2}$ mg/L)	Rising Time (s)	Settling Time (s)	$e_{ss,i} \times 10^{-2}$ (mg/L)
1	44.4	346.5	454.0	36.0
2	46.2	313.5	412.5	25.2
3	37.8	291.0	339.0	9.6
4	34.2	523.5	595.0	21.0
5	93.6	326.5	425.5	51.6
6	71.4	303.0	400.5	28.8
7	37.2	339.5	426.0	10.8
8	38.4	301.5	402.0	22.2
9	38.4	406.5	529.5	9.6
10	36.6	402.0	530.0	2.4
Average	47.4	355.4	451.4	21.6

3.2.2. Results of the PID Control Strategy

The second controller proposed in this work is the PID algorithm. In this case, the test bench operates under the same conditions as the previous controller. To apply the Ziegler–Nichols method, an input signal with amplitude $m = 100\%$ (Valve FV1 fully open) was considered, yielding the experimental reaction curve shown in Figure 10, where $L = 53$ s and $T = 2175.5$ s. Consequently, the proportional gain was determined as $k_p = 716.81$, with $T_i = 106$ s and $T_d = 26.5$ s, and these parameters were subsequently implemented in the PLC.

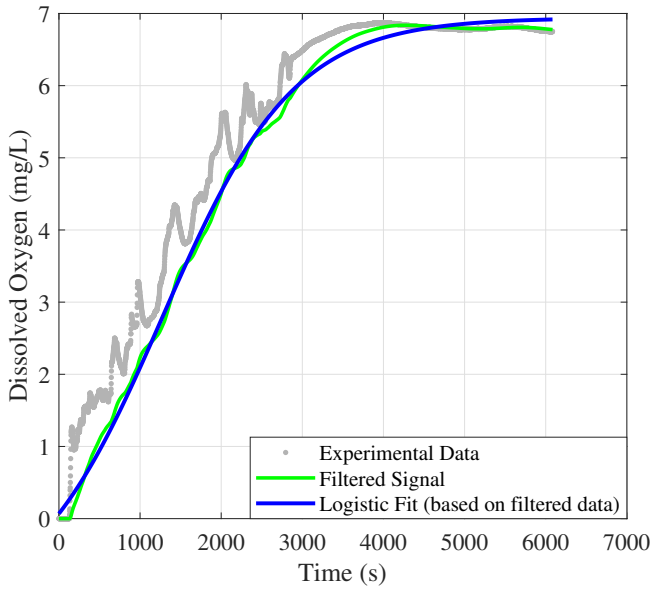


Figure 10. Measured, filtered, and sigmoidal-adjusted reaction curves of the DO signals (gray, green, and blue lines, respectively).

Figure 10 illustrates the system's reaction curve, as presented in Section 2.3.3. The gray dots represent the response to a step input until steady state, while the green line corresponds to the filtered data obtained using the discrete filter described in Equation (3). The adjusted sigmoidal reaction curve is shown as the blue line, derived from Equation (4).

Figures 11 and 12 illustrate the responses obtained by implementing the PID controller in the system. The setpoint remains at 6 mg/L, considering the same amount of sulfite in

the tank. Each test shows a minimum peak generated due to the reaction of the sulfite with dissolved oxygen when the aerator is activated. Compared with the On–Off, the responses do not exhibit oscillations, and the behavior is smoother.

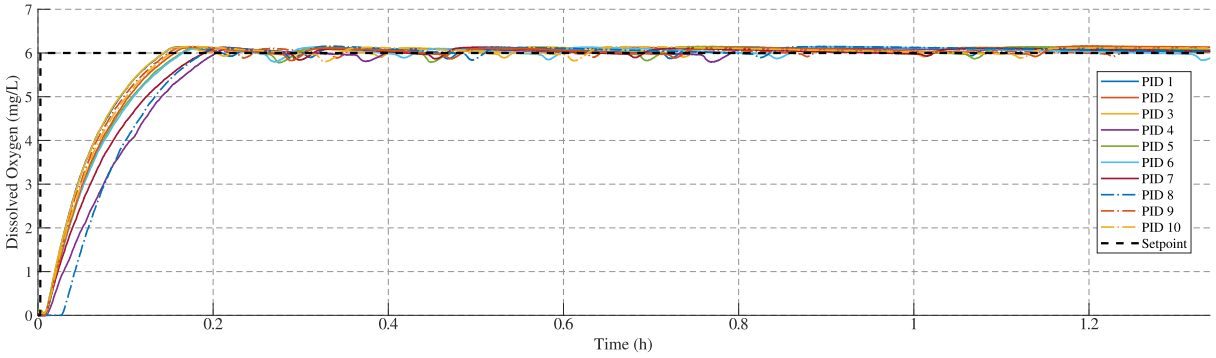


Figure 11. Dissolved oxygen responses obtained with PID control over 10 repetitions at a setpoint of 6 mg/L.

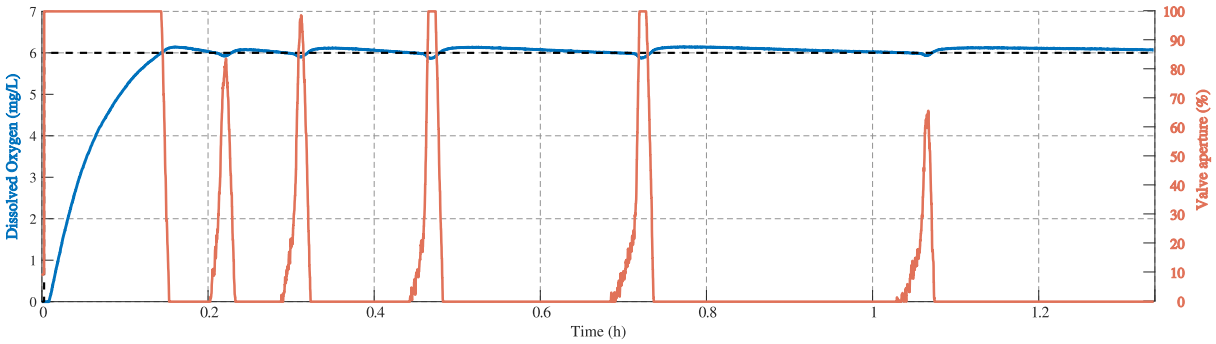


Figure 12. Corresponding valve aperture (orange line) for Test 1 under PID control (blue line) and reference (dashed line).

Table 3 presents the performance metrics of the PID implementation. The maximum overshoot is 42.6 $\times$ 10^{-2} (mg/L) at test 5; meanwhile, the minimum is 12 $\times$ 10^{-2} (mg/L) at test 4, with an average of 17.4 $\times$ 10^{-2} (mg/L). The average rising time is 394.3 s (0.11 h), with a maximum of 505 s recorded in test 4 and a minimum of 338.5 s recorded in test 3. In terms of settling time, the average is 521.5 s, with a maximum of 651 (test 4) and a minimum of 446.5 (test 3), respectively. Finally, the maximum mean error was observed in test 4, while the minimum was observed in test 9.

Table 3. Test results and average performance of the PID Control.

Test	Overshoot ($\times 10^{-2}$ mg/L)	Rising Time (s)	Settling Time (s)	$e_{ss,i} \times 10^{-2}$ (mg/L)
1	15.0	340.5	449.0	4.2
2	13.8	355.5	468.5	6.6
3	13.8	338.5	446.5	6.0
4	12.0	505.0	651.0	10.8
5	42.6	396.5	514.0	6.6
6	15.6	399.0	519.0	6.0
7	12.6	459.5	590.0	9.0
8	15.6	412.5	606.0	10.2
9	16.2	372.5	493.0	3.6
10	20.4	363.5	477.5	6.0
Average	17.4	394.3	521.5	7.2

The Z–N method was used as a standardized baseline; further fine-tuning was not pursued to keep methodology comparable and replicable. Therefore, these PID control results can be improved with more advanced tuning alternatives and other, more robust control strategies [31,36].

During the control tests, the PID controller shows lower steady-state error and variability under the tested conditions compared to the On–Off controller; see Table 4, particularly in the steady state. In the transient state, however, the settling time of both controllers is similar, since the PID controller saturates at 100% owing to the large error; see Figure 12. It is difficult to draw definitive conclusions in this regime, partly because it is further influenced by the residual sodium sulfite. In practical applications, however, it is the steady state that is most relevant.

Table 4. Summary of required repetitions and statistical indicators for each controller (95% confidence interval).

Controller	$N_{\min}$	$\bar{e}_{ss}$ (mg/L)	SE_N	h_N	Rel. Error (%)	$IC_{95\%}$ Rel. (%)
On–Off	8	0.2565	0.0482	0.1140	4.28	4.28 ± 1.90
PID	3	0.0560	0.0072	0.0310	0.93	0.93 ± 0.52

3.3. Numerical Evaluation of the Required Number of Repetitions

The confidence interval-based criterion was applied to the On–Off and PID controllers in order to determine the number of repetitions required for each case to obtain a reliable estimate of the steady-state mean error. The analysis follows the procedure described in Section 2.4. The required number of independent experimental repetitions was determined using a two-sided 95% confidence interval.

For each controller, the minimum N (number of tests) was selected such that the confidence interval semi-width $h_N = t_{0.975,N-1}\, SE_N$ satisfies the practical accuracy criterion $h_N \leq 0.02\, DO_d$, where $DO_d = 6$ mg/L is the reference value. This condition ensures that the estimation uncertainty remains within $\pm 2\%$ of the reference.

For the On–Off controller, the minimum number of repetitions satisfying this requirement was $N = 8$, whereas for the PID controller only $N = 3$ repetitions were required. Table 4 summarizes the corresponding steady-state error mean $\bar{e}_{ss}$, the standard error SE_N, the confidence semi-width h_N, and the relative error with respect to the reference.

It can be observed that, under the selected tuning and experimental conditions, the PID controller exhibits lower dispersion and therefore requires fewer repetitions to achieve the same statistical confidence level. However, this comparison should be interpreted as referential. Each controller may improve its performance and variability characteristics through further tuning adjustments. Consequently, the purpose of this analysis is not to establish a strict superiority of one control strategy over the other, but rather to illustrate a systematic and statistically grounded procedure for determining the sufficient number of experimental repetitions in each case.

3.4. Limitations and Future Work

This work intentionally avoids explicit system identification in order to maintain a simpler and more practical modeling approach, while remaining consistent with classical tuning procedures. However, this choice limits predictive simulation capabilities and reduces the generalizability of the results beyond the tested conditions. Future work should consider more rigorous black-box models (e.g., ARMAX) to better capture system dynamics and enable simulation-based evaluation and comparison of advanced control strategies prior to experimental implementation. A further limitation is the absence of a fully parameterized mechanistic model of the deoxygenation process, which would require

additional instrumentation to measure reaction and mixing dynamics not available in the present setup.

An interesting observation regarding DO regulation under On–Off control is that each oscillation exhibits a downward slope proportional to the residual sodium sulfite, as illustrated by the yellow dashed line in Figure 13 (left) following the initialization stage. Consequently, during the third oscillation, the variation in DO level becomes nearly constant, indicating that the sodium sulfite has been almost completely consumed. In other words, the disturbance generated in the aeration system due to the residual sodium sulfite is temporary, lasting on average three cycles in the steady state under On–Off control, although it is also expected to occur under PID control. Future work could focus on developing a methodology that not only reduces DO to its minimum value but also eliminates residual sodium sulfite prior to aeration control, thereby reducing the error variance observed in Figure 13 (middle and right).

Furthermore, in this study, we assumed that the amount of air supplied by the diffusers is proportional to the valve aperture. However, this relationship is not strictly linear in real applications. According to the technical specifications of both the air compressor and the diffusers, the dependence between these parameters is nearly linear across most operating ranges, but becomes nonlinear at the extremes. In future work, we suggest modeling this nonlinear behavior at the boundaries, using some data-based modeling method [26,37,38]. Moreover, data acquisition was carried out at a sampling frequency of 2 Hz ($T_s = 0.5$ s), which corresponds to the maximum rate permitted by the sensor. This rate can subsequently be reduced to lower the computational cost, where the minimum sampling rate value must satisfy the Nyquist criterion.

Finally, the results presented in this work encourage us to increase the complexity of the system by introducing disturbances into the system, such as varying the pond temperature or including living species in the tank. In addition, the aeration mechanism could be replaced with one that generates significant mass movement [12], so that new and more advanced control strategies can be studied on the platform proposed in this paper.

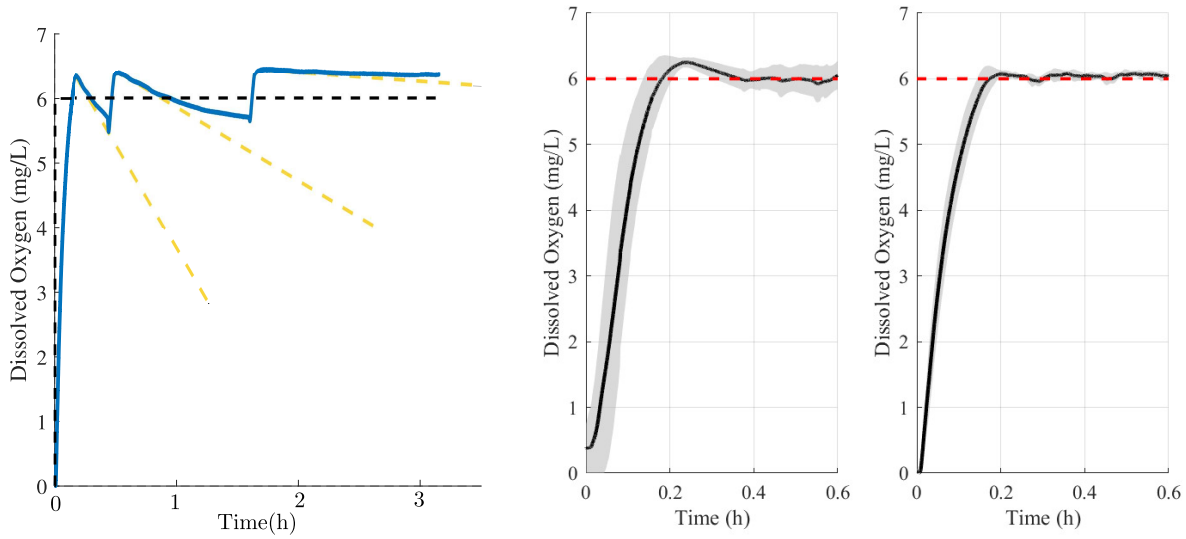


Figure 13. Long-term effect of residual sulfite during aeration: On–Off response (yellow dashed line, **left**), On–Off response with shaded variability band (**middle**), and PID response (**right**) with reference in 6 mg/L.

4. Conclusions

This paper presents a reproducible laboratory-scale benchmark for dissolved oxygen regulation that reduces environmental and biological variability while preserving the essen-

tial dynamics of aeration-based DO control. Beyond the comparison of control strategies, the main contribution of this work lies in the definition of a reproducible experimental framework and a statistically grounded methodology for performance evaluation. This approach enables more reliable benchmarking of control strategies prior to their deployment in real aquaculture systems. Using chemical deoxygenation to enforce comparable initial conditions, the platform enables statistically grounded comparison of two control strategies across repeated trials. The experiments show that On–Off control with hysteresis provides a simple and practically useful baseline, but results in considerable steady-state variability, whereas discrete-time PID achieves tighter regulation and smoother behavior under the same operating conditions. From an efficiency perspective, the smoother response achieved by the PID controller reduces unnecessary oscillations and actuator switching. This suggests a potential for reduced actuator cycling and energy use, which should be quantified in future work. Beyond highlighting performance differences, the proposed methodology makes it possible to determine how many repetitions are needed to reach a targeted confidence level in estimated tracking metrics, supporting more reliable controller evaluation prior to field deployment. Finally, the framework is positioned as a baseline for future extensions, including protocols that remove residual sulfite effects prior to control activation, inclusion of controlled disturbances such as temperature variation, and systematic testing of alternative aeration mechanisms and advanced strategies such as adaptive and predictive control.

Author Contributions: Conceptualization, J.M. and E.J.A.; methodology, J.M., S.P., A.G. and E.J.A.; software, J.M.; validation, J.M.; formal analysis, J.M. and E.J.A.; investigation, J.M. and E.J.A.; resources, J.M.; data curation, J.M.; writing—original draft preparation, J.M., S.P., A.G. and E.J.A.; writing—review and editing, J.M., S.P., A.G. and E.J.A.; visualization, J.M., S.P., A.G. and E.J.A.; supervision, E.J.A.; project administration, E.J.A.; funding acquisition, E.J.A. All authors have read and agreed to the published version of the manuscript.

Funding: This research was partially funded by CONCYTEC PROCIENCIA through the development of the Applied Research Projects Code E041-2023-02 (Contract No. PE501082364-2023) and Code E072-2024-01 (Contract No. PE501091923-2024), whose support contributed to the execution of this work.

Data Availability Statement: The data presented in this study are openly available at GitHub repository: https://github.com/jmagallanesc92/DO-Control accessed on 18 May 2026.

Conflicts of Interest: The authors declare no conflicts of interest.

References

1. Boyd, C.E. *Water Quality: An Introduction*; Springer: Cham, Switzerland, 2015. [CrossRef]
2. Boyd, C.E.; Tucker, C.S. *Pond Aquaculture Water Quality Management*; Springer: New York, NY, USA, 1998.
3. Yu, M.; Feng, Y.; Ouyang, B.; Wills, P.S.; Tang, Y. Dissolved oxygen in aquaculture ponds: Causal factors, predictive modeling, and intelligent monitoring. *Aquac. Eng.* **2026**, *112*, 102634. [CrossRef]
4. Wang, P.; Liu, H.; Zhao, S.; Yu, S.; Xie, S.; Hua, S.; Yan, B.; Xing, C.; Gao, H. Hypoxia stress affects the physiological responses, tissue damage and apoptosis in Litopenaeus vannamei. *Fish Shellfish. Immunol.* **2022**, *122*, 206–214. [CrossRef]
5. Nguyen, T.V.; Alfaro, A.C.; Rodríguez, J.; Bayot, B.; Sonnenholzner, S. Changes in metabolic profiling of whiteleg shrimp (*Penaeus vannamei*) under hypoxia stress. *J. Invertebr. Pathol.* **2022**, *193*, 107798. [CrossRef] [PubMed]
6. Jamaludin, M.; Tsai, Y.C.; Lin, H.T.; Huang, C.Y.; Choi, W.; Chen, J.G.; Sean, W.Y. Modeling and Control Strategies for Energy Management in a Wastewater Center: A Review on Aeration. *Energies* **2024**, *17*, 3162. [CrossRef]
7. Ren, Q.; Wang, X.; Li, W.; Wei, Y.; An, D. Research of dissolved oxygen prediction in recirculating aquaculture systems based on deep belief network. *Aquac. Eng.* **2020**, *90*, 102085. [CrossRef]
8. Zhou, X.; Wang, J.; Huang, L.; Li, D.; Duan, Q. Modelling and controlling dissolved oxygen in recirculating aquaculture systems based on mechanism analysis and an adaptive PID controller. *Comput. Electron. Agric.* **2022**, *192*, 106583. [CrossRef]

9. Jayanthi, M.; Balasubramaniam, A.; Suryaprakash, S.; Veerapandian, N.; Ravisankar, T.; Vijayan, K. Assessment of standard aeration efficiency of different aerators and its relation to the overall economics in shrimp culture. *Aquac. Eng.* **2021**, *92*, 102142. [CrossRef]
10. Colt, J. *Computation of Dissolved Gas Concentrations in Water as Functions of Temperature, Salinity and Pressure*; American Fisheries Society Special Publication; American Fisheries Society: Bethesda, MD, USA, 1984; Volume 14, pp. 1–154.
11. APHA. *Standard Methods for the Examination of Water and Wastewater*, 23rd ed.; American Public Health Association: Washington, DC, USA, 2017.
12. Cahua, D.; Antezana, F.; Palomino, S.; Alegria, E.J. Prototype Aeration System for Dissolved Oxygen Control Using a Paddle Wheel Mechanism. In Proceedings of the 2025 16th IEEE International Conference on Industry Applications (INDUSCON), São Sebastião, Brazil, 14–17 October 2025; pp. 16–21. [CrossRef]
13. Rastegari, H.; Nadi, F.; Lam, S.S.; Ikhwanuddin, M.; Kasan, N.A.; Rahmat, R.F.; Mahari, W.A.W. Internet of Things in aquaculture: A review of the challenges and potential solutions based on current and future trends. *Smart Agric. Technol.* **2023**, *4*, 100187. [CrossRef]
14. Singh, M.; Sahoo, K.S.; Gandomi, A.H. An Intelligent-IoT-Based Data Analytics for Freshwater Recirculating Aquaculture System. *IEEE Internet Things J.* **2024**, *11*, 4206–4217. [CrossRef]
15. Badiola, M.; Mendiola, D.; Bostock, J. Recirculating Aquaculture Systems (RAS) analysis: Main issues on management and future challenges. *Aquac. Eng.* **2012**, *51*, 26–35. [CrossRef]
16. Timmons, M.B.; Ebeling, J.M. *Recirculating Aquaculture*, 4th ed.; Cayuga Aqua Ventures: Ithaca, NY, USA, 2018.
17. Zhou, X.; Li, D.; Zhang, L.; Duan, Q. Application of an adaptive PID controller enhanced by a differential evolution algorithm for precise control of dissolved oxygen in recirculating aquaculture systems. *Biosyst. Eng.* **2021**, *208*, 186–198. [CrossRef]
18. Durdevic, P.; Raju, C.S.; Yang, Z. Potential for Real-Time Monitoring and Control of Dissolved Oxygen in the Injection Water Treatment Process. *IFAC-PapersOnLine* **2018**, *51*, 170–177. [CrossRef]
19. Kwon, H.J.; Jeong, J.S. Clearing up the oxygen dip in HPAEC–PAD sugar analysis: Sodium sulfite as an oxygen scavenger. *J. Chromatogr. B* **2019**, *1128*, 121759. [CrossRef]
20. Zhao, B.; Li, Y.; Tong, H.; Zhuo, Y.; Zhang, L.; Shi, J.; Chen, C. Study on the reaction rate of sulfite oxidation with cobalt ion catalyst. *Chem. Eng. Sci.* **2005**, *60*, 863–868. [CrossRef]
21. Porfert, C. *QA Bulletin: Calibration of Dissolved Oxygen Meters*; Technical Report EQAGUI-DO, Revision 0; United States Environmental Protection Agency (EPA) New England, Office of Environmental Measurement and Evaluation, Quality Assurance Unit: North Chelmsford, MA, USA, 2006.
22. Bedner, M.; MacCrehan, W.A.; Helz, G.R. Making chlorine greener: Investigation of alternatives to sulfite for dechlorination. *Water Res.* **2004**, *38*, 2505–2514. [CrossRef]
23. Moore, N.; Ebrahimi, S.; Zhu, Y.; Wang, C.; Hofmann, R.; Andrews, S. A comparison of sodium sulfite, ammonium chloride, and ascorbic acid for quenching chlorine prior to disinfection byproduct analysis. *Water Supply* **2021**, *21*, 2313–2323. [CrossRef]
24. Li, X.; Zhao, Z.; Qu, Z.; Li, X.; Zhang, Z.; Liang, X.; Chen, J.; Li, J. A Review of Traditional and Emerging Residual Chlorine Quenchers for Disinfection Byproduct Research. *Toxics* **2023**, *11*, 410. [CrossRef]
25. Proakis, J.G.; Manolakis, D.G. *Digital Signal Processing: Principles, Algorithms, and Applications*, 5th ed.; Pearson Education: Hoboken, NJ, USA, 2022.
26. Alegria, E.J.; Bottura, C.P. Data-Based Local Smoothing Technique for Parameters Estimation of Nonlinear ARX Models. In Proceedings of the 2019 American Control Conference (ACC), Philadelphia, PA, USA, 10–12 July 2019; pp. 4350–4355. [CrossRef]
27. Han, H.; Tang, Z.; Li, H.; Yang, H.; Wu, X. Robust inverse control strategy for dissolved oxygen concentration based on disturbance boundary estimation. *Int. J. Robust Nonlinear Control* **2024**, *Online Version of Record*. [CrossRef]
28. Yao, X.; Zhang, G.; Yang, S.; Chen, Y. Adaptive Anti-Disturbance Control of Dissolved Oxygen in Circulating Water Culture Systems. *Symmetry* **2023**, *15*, 2015. [CrossRef]
29. Quispe, M.; Chiotti, D.; Del-Águila, J.; Quino, G.; Jara Alegria, E. Automatic pellet positioner with switched fuzzy-PD control for a smart shrimp feeder. *Smart Agric. Technol.* **2026**, *13*, 101863. [CrossRef]
30. Chiotti, D.; Quispe-Carlos, M.; Quino, G.; Jara Alegria, E. Control Strategies for an Aquaculture Feeder on an Oscillating Platform Using Disturbance-Based Weight Estimation. *Electronics* **2026**, *15*, 973. [CrossRef]
31. Ogata, K. *Modern Control Engineering*, 5th ed.; Prentice Hall: Upper Saddle River, NJ, USA, 2010.
32. Ziegler, J.G.; Nichols, N.B. Optimum Settings for Automatic Controllers. *Trans. ASME* **1942**, *64*, 759–768. [CrossRef]
33. Franklin, G.F.; Powell, D.; Emami-Naeini, A. *Feedback Control of Dynamic Systems*, 8th ed.; Pearson: Harlow, UK, 2019.
34. Montgomery, D.C.; Runger, G.C. *Applied Statistics and Probability for Engineers*, 7th ed.; John Wiley & Sons: Hoboken, NJ, USA, 2018.
35. Box, G.E.P.; Hunter, J.S.; Hunter, W.G. *Statistics for Experimenters: Design, Innovation, and Discovery*, 2nd ed.; Wiley-Interscience: Hoboken, NJ, USA, 2005.

36. Borase, R.P.; Maghade, D.K.; Sondkar, S.Y.; Pawar, S.N. A review of PID control, tuning methods and applications. *Int. J. Dyn. Control* **2021**, *9*, 818–827. [CrossRef]
37. Alegria, E.J.; Giesbrecht, M.; Bottura, C.P. Causal regression for online estimation of highly nonlinear parametrically varying models. *Automatica* **2021**, *125*, 109425. [CrossRef]
38. Alegria, E.; Giesbrecht, M.; Bottura, C. An associative-memory-based method for system nonlinearities recursive estimation. *Automatica* **2022**, *142*, 110343. [CrossRef]

Disclaimer/Publisher's Note: The statements, opinions and data contained in all publications are solely those of the individual author(s) and contributor(s) and not of MDPI and/or the editor(s). MDPI and/or the editor(s) disclaim responsibility for any injury to people or property resulting from any ideas, methods, instructions or products referred to in the content.